Calibration and Multiple Views

Camera Calibration From Spheres Images

N.Daucher, M.Dhome, J.T.Lapresté

LASMEA, URA 1793 du CNRS
Université Blaise Pascal, 63177 AUBIERE CEDEX (FRANCE)
Tél : 73.40.72.32, fax 73.40.72.62, email: daucher@le-eva.univ-bpclermont.fr

Abstract

From spheres images we have developed a new method for camera calibration in order to calculate with accuracy its intrinsic parameters. We prove an interesting geometric propriety about ellipses extracted from sphere images. Taking into account the lens geometrical distortion introduced by the optical system and searching a precise points detection for spheres images, permit to obtain satisfactory results.

1 Introduction

Prior to the analysis of images obtained from a camera and digitization system, it is necessary, if one plans to use the system as a measurement device, to calibrate it.

Camera calibration remains a crucial topic on which many searchers have already worked. Commonly, calibration involves two kinds of parameters:
- intrinsic ones: related to the device geometry.
- extrinsic ones: related to the relative pose of the calibration target and the device.

A first approach consists in determining in one global pass, all these parameters from the matching of a set of points defined on the calibration target with their projections on the image plane [10] [6] [7]. Another one consists in computing successively intrinsic and extrinsic parameters, using particular geometrical properties as (for instance) those of vanishing points of orthogonal pencils of parallel straight lines in space [11] [7].

Generally, these methods, opposite to those of photogrammeters, do not take account of optical distortion phenomenons related to the camera lens. As they also are very sensitive to the detection accuracy of the image primitives used by the calibration process, they can produce poor results.

We have chosen to keep the second approach, trying to limit its drawbacks. The calibration target is a mere sphere. The computation of the intrinsic parameters is done from multiple views of the same sphere. The image primitives are the ellipses that are the projections of the sphere limb points.

Our method is based on a geometrical property of this kind of primitive (see 2.2.1). The choice of such images is justified by the following facts:

- The great number of contour points belonging to one primitive permits its accurate determination.

- Points belonging to the sphere limb are all situated at the same distance of the optical center and thus are enjoying the same sharpness for a given focus.

- Moreover, this kind of primitives (as we shall see) permits to get partly rid of the distortion problems, if it is possible to consider that distortion is radial from the intersection point between the image plane and the optical axis.

2 Mathematical background

Our aim is to compute the four intrinsic parameters of a camera device. These are:

- coordinates (u_0, v_0) of the intersection of the image plane with the optical axis. This point will be referred in the sequel as the 'image principal point'.

- the ratio $k = dy/dx$ of the digitization steps of the acquisition system.

- the focal length f of the camera.

Lecture Notes in Computer Science, Vol. 800
Jan-Olof Eklundh (Ed.)
Computer Vision – ECCV '94

2.1 Computation method

Let us recall that limb points of a surface are points where the tangent plane goes through the camera optical center. The computation is based on the following property of the limb points of a sphere:

Theorem : *The projection of the limb points of a sphere is an ellipsis the great axis of which goes through the principal point* $(u0, v0)$ *, intersection of the optical axis with the image plane.*

The details of the proof of this assertion can be found in [12]. In fact, we use the equations of the two axes and minimize the product of the distances of the principal point to each of the main axes. This quantity (denoted *prodist*) is expressed as following:

$$(1) \qquad prodist = D y_c - E x_c = \frac{1}{AC - B^2}(D(BD - AE) - E(BE - CD))$$

where (x_c, y_c) are the coordinates of the ellipsis center, and (A, B, C, D, E) are the coefficients of the ellipsis equation expressed in the camera frame[1]. These are related to the coefficients (A', B', C', D', E') of the ellipsis equation expressed in the natural image frame[2] by the following relations:

$$\begin{cases} A = A'/\mathrm{dx}^2 \\ B = B'/\mathrm{dxdy} \\ C = C'/\mathrm{dy}^2 \end{cases} \qquad \begin{cases} D = (D' + B'v_0 + A'u_0)/\mathrm{dx} \\ E = (E' + B'u_0 + C'v_0)/\mathrm{dy} \\ F = F' + 2E'v_0 + 2D'u_0 + C'v_0^2 + 2B'u_0v_0 + A'u_0^2 \end{cases}$$

These relations permit to express *prodist* in terms of the intrinsic camera parameters, and of the coefficients of the ellipsis detected in the image.

It appears that the last intrinsic parameter (the focal length) can also be analytically computed.

$$f = \sqrt{\frac{(B/DE) - 1}{(AB/DE) - (B/E)^2}}$$

3 Calibration problem solving

The estimation of the camera intrinsic parameters will be done in two steps:

3.1 First step:

We shall compute first $u_0, v_0, k = \mathrm{dy}/\mathrm{dx}$ by zeroing the product of the distances from the point (u_0, v_0) to the two main axes of the detected ellipsis.

This product is zeroed if and only if $N = D(BD - AE) - E(BE - CD) = 0$. We use a first order development of N quantity and iterative Newton-Raphson's approach.

3.2 Second step:

The computation of the focal length, if it remains simple in its analytical form, only depends of the ellipses coefficients. On synthetic images, one ellipsis is sufficient to determine exactly the focal length. If noise is added to these images, it appears that these coefficients and the whole focal computation is badly conditioned, and the result is not so good. Thus, the focal length is determined using the mean value of the focal lengths associated to each ellipsis.

Moreover, we cannot really escape from the image distortion phenomena which is common to all optical systems. The data given by the constructor of the used system of lenses indicate a radial distortion. This radial distortion does not really affect the determination of the first three parameters; if it is clear that radial distortion leads to approximate curves, that are no more real ellipses, by an ellipsis equation, it must be noted that the distortion preserves the figure symmetry around the great axis that goes through

---

1 orthonormal centered at the optical center.

2 related to the camera frame by the relations: $u = x/\mathrm{dx} + u_0$, $v = y/\mathrm{dy} + v_0$,

(u_0, v_0). Consequently the approximating ellipsis we compute must share the axis of the ideal ellipsis (without distortion). This is proved (see 4.1.1) by experiments on synthetic images.

If this distortion is not a prejudice to our method for determining u_0, v_0, k, the same can not be said for the focal length as the distortion modifies image dimensions. It is thus mandatory to correct the contour points before computing the focal length. We have developed a reliable software method to compute and correct the radial distortion from grid images. It is the one we use for correcting our spheres images. You can refer to [9] to find details about this work.

The second factor that acts on the determination of the focal length is the localization of limb points. The next section explains the principle of their determination.

3.3 Sphere limb Localization

The commonly retained definition of contour points in a brightness image can be stated as following:

Definition :

Contours points in a brightness image are situated where the modulus of the gradient vector is:
1 - big enough.
2 - locally maximal in the gradient vector direction.

Many interesting algorithms are based on this definition, in particular those of R. Deriche [5] or J.S. Chen [4]. The limb points being the points where the surface normal is orthogonal to the projection direction are de facto dark points where the grey level is small. We have tried to extract points corresponding to the beginning of the front of the camera output; these points are in fact maximal curvature points and we used R. Deriche gradient computation algorithm successively to the grey level image and then to the image of the gradient modulus obtained from the first pass. On this last image the local maxima are extracted.

4 Experiments

Experiments on synthetic images have been done in order to confirm the theoric approach previously developed. These experiments show advantages but also limits of the method. The experiments on real images permit us to validate our method.

4.1 Synthetic images

We have built synthetic 512x512 images as the projection of the limb points of a sphere whose radius value is 3cm, situated at 0.8m, 1m and 1.2m in front of the camera and for respectively 1500 pixels, 2000 pixels, 2500 pixels focal lengths. The principal point position in the image is $(u_0, v_0) = (255,255)$ and digitization ratio $k = 1$. The radial distortion is modelled as [2]:

$x_d = x(1 + k_1 r^2 + k_2 r^4)$
$y_d = y(1 + k_1 r^2 + k_2 r^4)$

with:
(x, y) : coordinates of a point in the undistorted image
(x_d, y_d) : coordinates of the same point in the distorted image
r : distance from point (x, y) to the image center (u_0, v_0)
k_1, k_2 : radial distortion coefficients.

4.1.1 First experiments set: showing the no influence of radial distortion on u_0, v_0, k calculation

The tables below show an example of great axis convergence for undistorted and distorted images with distortion coefficients $k_1 = 10^{-6}$, $k_2 = 10^{-12}$, without noise and with an 1/10 pixel added noise on each image point.

without noise, without distortion

	f=1500	f=2000	f=2500
u_0	255.000	255.000	255.000
v_0	255.000	255.000	255.000
k	1.000	1.000	1.000

noise=1/10 px,without distortion

	f=1500	f=2000	f=2500
u_0	255.090	258.803	258.626
v_0	252.778	249.692	238.971
k	1.000	0.999	0.999

without noise, $k1 = 10^{-6}, k2 = 10^{-12}$

	f=1500	f=2000	f=2500
u_0	254.999	255.000	255.008
v_0	255.000	254.999	254.986
k	1.000	1.000	1.000

noise=1/10 px, $k1 = 10^{-6}, k2 = 10^{-12}$

	f=1500	f=2000	f=2500
u_0	254.867	254.772	255.239
v_0	255.899	255.869	254.459
k	1.001	1.001	0.999

Considering these tables, we can notice that the results are not affected by the radial distortion either on noised or unnoised images, whatever the focal length used. However, on undistorted images (i.e. corrected images), the greater the focal length is the more important the noise influence is; this fact is explained by a smaller perspective effect for a long focal length than for a short one; the sphere image being thus nearly circular it is more difficult to determine the ellipsis axis and so the parameters computation accuracy decreases.

On real images we shall be well advised to estimate the u_0, v_0, k parameters from not corrected images.

4.1.2 Second experiments set: showing the influence of a points detection on the focal length calculation

This figure shows the contour obtained in a classical way, looking for local maxima with the Deriche algorithm used on the grey level image (internal contour) and the contour obtained by applying the Deriche algorithm to the modulus of gradient image (external contour). The two contours are superimposed on the corresponding brightness image.A displacement of the contours can be observed toward the image borders.

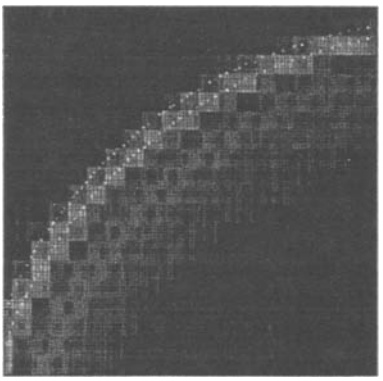

For each synthetic ellipsis point, we have added 3 pixels to its distance from the ellipsis center. Thus we obtain an image concentric to the initial image as showing on the above figure.

The focal length computation is done by computing the mean value of the set of all the obtained values. So it appears a 2,5% error in comparison with the theoretical value. The noise influence is essentially on the standard deviation associated to the focal length mean value. As it could be expected, the smaller the standard deviation is, the shorter the focal length is, for the same reasons than explained above (about the perspective effect), because the focal expression is only depending of ellipsis parameters in the camera frame (whose accuracy is itself depending of a good knowledge of (u_0, v_0, k)).

4.2 Real images

Figure 7 presents the experimental layout.

The used sphere is a snooker ball on the center of a mask surrounded by a circular neon lighting. We have chosen these lighting conditions to have uniform lighting and minimize diffusion on the limb points. For a fixed focus of the camera, multiple images of this sphere scattered around the optical axis direction were acquired.

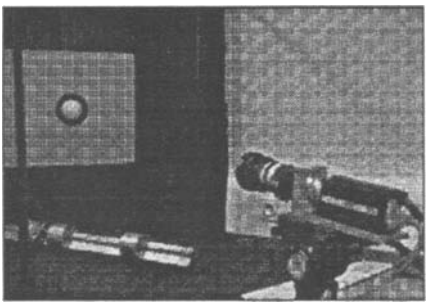

Figure 7: Experimental layout.

4.2.1 Results

The whole calibration process have been tested for three sets of sphere and grid associated images, i.e. for three focus distances and three focal length values. The following images show the axes convergence into (u_0, v_0).

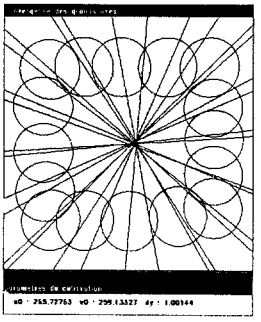

S1

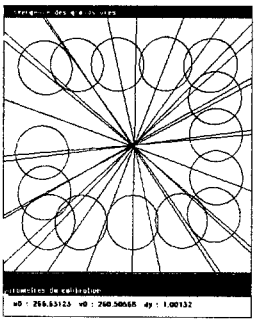

S2

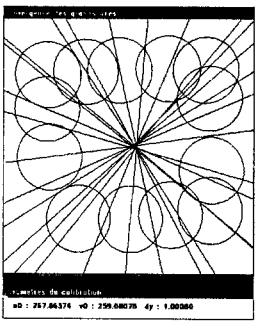

S3

The following table sums up some obtained results:

Sets	u_0 (pixels)	v_0 (pixels)	k	computed focal length (mm)	manufacturer focal length (mm)
S1	267,53	258,08	0,999	23,97±3,12	~22,54
S2	265,16	258,27	0,999	31,88±7,02	~29,85
S3	263,88	263,77	1,001	38,09±14,78	~40,47

-*computed focal length*: value computed with our method.

-*manufacturer focal length*: theoretical value given by ANGENIEUX.

This last value is obtained using the set of tables given by the lens manufacturer (ANGENIEUX). From the value of the lens and the focus distance graduations, these tables give a theoretical focal length value. Of course, this value is depending of the reading accuracy on the graduations and can be only used as a point of reference.

If we compare the computed focal length values with theoretical ones, these can be considered as correct concerning the mean value. However as for the synthetic images the longer the focal length is the greater the standard deviation is.

As we consider our method of radial distortion correction as reliable [9], we think that work has still to be done in order to increase the accuracy of the points detection in the images to improve the focal length determination accuracy.

5 Conclusion

This new calibration method, even if it is one more in a bunch of old and new ones [1], does not look so uninteresting.

First, we have chosen to take advantage of image primitives that have been , up to now, seldom used in camera calibration. The points of interest in a sphere image are numerous and share a common sharpness. The ellipsis equation (from where they belong) can be accurately computed. Moreover, the geometrical property used is relatively insensitive to the lens radial distortion.

Our method allows to simply determine the coordinates of the point of intersection between the optical axis of the camera and the image plane (u_0, v_0) as well as the ratio of the digitizing steps (dy/dx).

Focal length determination is more sensitive, even if its mathematical formulation is very simple.

In fact, at least two factors are present to spoil the dimension and shape of images. Firstly, accuracy of contour points detection, secondly geometric distortion from acquisition system. If it is possible to correct the distortion, accuracy in computing limb points of a sphere is a rather delicate problem. Our approach, which could be improved, gives results that can be judged as good : they have been validated by comparison with theorical data .

Finally, it can be said that the results of this new method to determine intrinsic camera parameters are satisfactory. One of its main advantages of the method is the simplicity of use both in real utilisation and mathematical formulation.

References

[1] P.Beardsley, D.Murray, A.Zisserman. Camera Calibration Using Multiple Images, In *Proceedings of ECCV '92*, Santa Margherita Ligure, Italie, Mai 92, pages 312-320.

[2] H.Beyer. Geometric and Radiometric Analysis of a CCD-Camera Based Photogrammetric Close-Range System, *Institut für Geodäsie und Photogrammetrie, Dissertation ETH n°9701*, Zürich, May 1992.

[3] C.Cagnac, E.Ramis, J.Commeau, *Nouveau cours de Mathématiques Spéciales vol n°3 géométrie*, éditions Masson & Cie, 1965.

[4] J.S. Chen and G.Medioni. Detection, Localization and Estimation of Edges. In *Proceedings of IEEE Workshop on Computer Vision*, Miami, November 1987, pages 215-217.

[5] R.Deriche, Optimal Edge Detection Using Recursive Filtering,*In Proceedings of First ICCV*, Londres, Juin 1987, pages 501-505.

[6] O.Faugeras et G.Toscani, Camera Calibration for 3D Computer Vision,*In Proceedings of International Workshop on Machine Intelligence*, Tokyo, Février 1987.

[7] P.Limozin-Long, Présentation et Comparaison de trois méthodes de calibration, *Convention de recherche ESA/INRIA*, Février 1988.

[8] H.Press, B.Flannery, Teukolsky S., Vetterling W., *Numerical Recipes, The Art of Scientific Computing*, pages 52-64.

[9] S.Rémy, M.Dhome, N.Daucher, J.T.Lapresté, *Estimation de la distorsion radiale d'un système optique*, Actes du 9ème Congrès RFIA de l'AFCET, Janvier 94, Paris, pages 99-108.

[10] R.Y Tsaï, An Efficient and Accurate Camera Calibration Techniques for 3D Machine Vision, *In Proceedings of Computer Vision and Pattern Recognition*, Miami, Juin 1986, pages 364-374.

[11] G.Q. Wei, Z.Y He and S.D MA, Camera Calibration for Stereo Vision by Vanishing Points, *Second Joint China-France Conference on Robotics*, Paris, 5-6-7 Décembre 1988.

[12] N.Daucher, M.Dhome, J.T. Lapresté, *Camera Calibration From Spheres Images*, Technical Report, 1993.